ANNUAL REVIEWS

Annual Review of Physical Chemistry

Single-Molecule Spectroscopy and Super-Resolution Mapping of Physicochemical Parameters in Living Cells

Megan A. Steves, Changdong He, and Ke Xu

Department of Chemistry, University of California, Berkeley, California, USA; email: xuk@berkeley.edu

Annu. Rev. Phys. Chem. 2024. 75:163–83

First published as a Review in Advance on February 15, 2024

The *Annual Review of Physical Chemistry* is online at physchem.annualreviews.org

https://doi.org/10.1146/annurev-physchem-070623-034225

Keywords

multidimensional super-resolution microscopy, single-molecule spectroscopy, functional imaging, intracellular physicochemical parameters, spectral microscopy, spatial mapping

Abstract

By superlocalizing the positions of millions of single molecules over many camera frames, a class of super-resolution fluorescence microscopy methods known as single-molecule localization microscopy (SMLM) has revolutionized how we understand subcellular structures over the past decade. In this review, we highlight emerging studies that transcend the outstanding structural (shape) information offered by SMLM to extract and map physicochemical parameters in living mammalian cells at single-molecule and super-resolution levels. By encoding/decoding high-dimensional information—such as emission and excitation spectra, motion, polarization, fluorescence lifetime, and beyond—for every molecule, and mass accumulating these measurements for millions of molecules, such multidimensional and multifunctional super-resolution approaches open new windows into intracellular architectures and dynamics, as well as their underlying biophysical rules, far beyond the diffraction limit.

1. INTRODUCTION

Recent advances in super-resolution (fluorescence) microscopy (SRM) based on the massive accumulation of the superlocalized positions of single molecules that stochastically switch between emitting and dark states over different camera frames, i.e., single-molecule localization microscopy (SMLM), have led to exciting scientific discoveries and technical developments (1–6). Many existing reviews on SMLM and SRM focus on the ever-increasing spatiotemporal resolutions, aiming to elucidate subcellular structural (shape) information to the best possible extent.

In this review, we focus on emerging work that transcends the outstanding structural information offered by SMLM to extract and map functional (7) physicochemical parameters in living mammalian cells at single-molecule and super-resolution levels. While such experiments are often enabled by encoding/decoding new dimensions of the single-molecule signal, they are also distinct from earlier single-molecule spectroscopy (SMS) studies in which isolated events are recorded (8–11). Instead, to achieve mapping at the nanoscale, SMSs of various forms are mass accumulated, often for millions of individual molecules, to be integrated with the superlocalized positions of the same molecules. Below we categorize our discussion by the different single-molecule signal spaces being probed, including fluorescence intensity, spectra, motion, polarization, lifetime, and nonfluorescence methods. Together, these rising multidimensional SRM approaches afford rich spatial and functional information and hence exciting new insights into the dynamic processes and behaviors of living cells.

2. SINGLE-MOLECULE FLUORESCENCE INTENSITY

The fluorescence intensity remains the most straightforward parameter to analyze in single-molecule data. However, owing to the inherently large molecule-to-molecule variation in the emission intensity in SMLM, small changes in intensity are difficult to discriminate. Fluorescence turn-on of initially dark probes offers a strategy to map physical parameters or chemical activities by counting the locally activated molecules. Still, such approaches leave ambiguities between the local level of activation and concentration of probes, hence a blurred boundary between functional and structural readouts. This issue may be overcome with fluorescence spectrum and lifetime detections, which are discussed in Sections 3 and 6.

2.1. Fluorescence Turn-On Owing to Specific Local Environments and Protein Conformations

A class of fluorogenic probes turn on when entering specific physical environments (12). For example, the solvatochromic dye Nile red is nonfluorescent in aqueous solutions but becomes highly emitting in hydrophobic environments. This effect provides a mechanism in which dynamic single-molecule fluorescence on-off switching is maintained over long periods as probe molecules stochastically enter and exit the hydrophobic phase (**Figure 1*a***), hence enabling SMLM for in vitro and cellular lipid membranes (**Figure 1*b***) (13–16) and in vitro protein aggregates (15, 17–19). The fluorescence quantum yield of rotatable molecules can be strongly enhanced by conformation locking. For functional SMLM, such effects have enabled the detection and SRM imaging of specific protein conformations, e.g., β-sheet aggregates in amyloid fibrils (19–24). Beyond the passive binding of fluorogenic probes, Liu et al. (25) devised biosensors in which, upon protein conformation changes, a concealed small tag is exposed to bind with a fluorescent reporter. They thus detected single active proteins and tracked their motion in the live-cell plasma membrane.

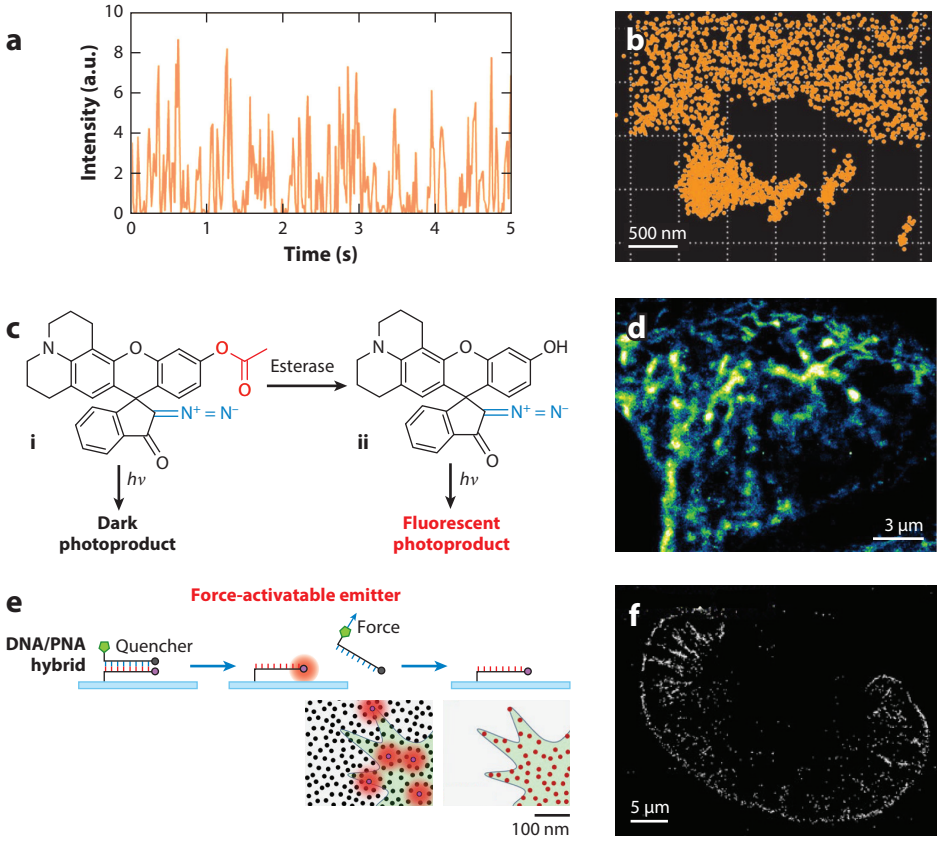

Figure 1

SMLM via fluorescence turn-on from specific local environments, reactions, and engineered biomolecular interactions. (*a*) Fluorescence intensity time trace for a lipid vesicle, showing bursts due to the stochastic entering of single Nile red molecules into the lipid phase from the aqueous medium. (*b*) SMLM image of a supported lipid bilayer obtained by localizing 2,778 single Nile red molecules over 4,095 frames due to the fluorescence turn-on process in panel *a*. (*c*) Schematic of a caged (initially dark) probe (*i*) that can be photoactivated into a fluorescent state after removal of the acetyl group by carboxylesterases (*ii*). (*d*) SMLM image of esterase activity based on subpanel *i* in panel *c* in a live mammalian cell. (*e*) Schematic of cellular force SMLM based on force-activatable emitters in which the unzipping of a DNA/peptide nucleic acid (PNA) hybrid leads to fluorescence dequenching and single-molecule emission. (*f*) Resultant integrin molecular tension SMLM of a migrating keratocyte from 20 frames of recording. Abbreviation: SMLM, single-molecule localization microscopy. Panels *a* and *b* adapted from Reference 13; copyright 2006 National Academy of Sciences. Panels *c* and *d* adapted with permission from Reference 27; copyright 2017 American Chemical Society. Panels *e* and *f* adapted with permission from Reference 32; copyright 2020 American Chemical Society.

2.2. Reaction-Triggered Fluorescence Turn-On

Initially caged or quenched fluorophores may be turned on by chemical or enzymatic reactions (26), thus opening a window into local activities. For SMLM, Halabi et al. (27) devised a fluorogenic probe that was activated by carboxylesterases (**Figure 1*c***), and thus reconstructed SRM images of esterase activity in live cells (**Figure 1*d***). Chai et al. (28) developed a β-galactosidase (β-Gal)-responsive photochromic fluorescent probe, enabling SMLM mapping of the subcellular distribution of β-Gal activity.

The fluorophore intensity may also be modulated by ion binding/unbinding. Fluorescent indicators have thus been employed to visualize local bursts of pH and Ca^{2+} signals in live cells. Treating individual bursts—presumably owing to the collective responses of indicator molecules to individual subdiffraction-limit events, e.g., synaptic vesicle activities, analogous to single-molecule images in SMLM—thus allowed the super-resolution visualization of activity hot spots (29–31).

2.3. Fluorescence Turn-On and Fluctuation via Interactions Between Biomolecules

Fluorescence turn-on and fluctuation may also be engineered via interactions between biomolecules. Based on the tension-induced unzipping of DNA structures, two recent studies employed fluorescent probes that were activated by the piconewton traction forces between single integrin proteins at the cell surface and the substrate, and so achieved SMLM force mapping (e.g., **Figure 1*e*,*f***) (32, 33). With split fluorescent proteins (FPs), bimolecular fluorescence complementation has been successfully integrated with SMLM to map protein-protein interactions in live cells (34, 35). Meanwhile, fluorescence fluctuation increase by contact (FLINC) capitalizes on the elevated fluctuations in the fluorescence intensity when two FPs are brought into proximity, thus achieving SRM of enzyme activities in live cells (36, 37).

3. SINGLE-MOLECULE SPECTRAL RESPONSES

Spectral responses provide a robust way to encode functional information that is decoupled from the fluorescence intensity and count of single molecules. Although it has been technically demanding to extract the spectral characteristics of single molecules, recent years have seen the emergence of new approaches that well suit the unique operational schemes of SMLM.

3.1. Wavelength-Split Detection

A facile method to detect single-molecule spectral responses is wavelength-split detection, in which a dichroic mirror splits (wide-field) fluorescence into two views for the separate, parallel recording of long- and short-wavelength components (**Figure 2*a***). For SMLM, this approach enables the identification of single molecules based on the ratio of the detected photon counts in the two views (**Figure 2*b***). With a single excitation laser, multicolor SMLM is thus concurrently performed for two to four fluorophores of overlapping spectra (e.g., **Figure 2*c***) (38–40). For imaging functional parameters, the local pH has been examined in gel and silica systems through the two-wavelength ratiometric single-molecule detection of SNARF-1, a fluorescent pH indicator that exhibits substantially different emission spectra in its protonated and deprotonated states, so far limited to sparse molecules (41, 42).

Wavelength-split detection schemes have also been vital to Förster resonance energy transfer (FRET) experiments in which the relative emission intensities of donor and acceptor fluorophores serve as a molecular ruler for quantifying interactions and conformational dynamics at sub-10-nm length scales (43, 44). Chemically synthesized and genetically encoded FRET-based biosensors have elucidated vital functional parameters inside the living cell, including ion and small-molecule concentrations, cellular microenvironments, and enzymatic activities (45, 46).

Single-molecule FRET (smFRET) offers powerful insights into parameters obscured in ensemble averaging, e.g., multiple states and their interconversions, and so has become an indispensable tool for studying biomolecular conformations and dynamics in vitro (44, 47, 48). However, smFRET has seen limited applications in live cells (44, 49). The relatively low brightness and large size of FPs make them unfavorable for smFRET; various approaches have thus been

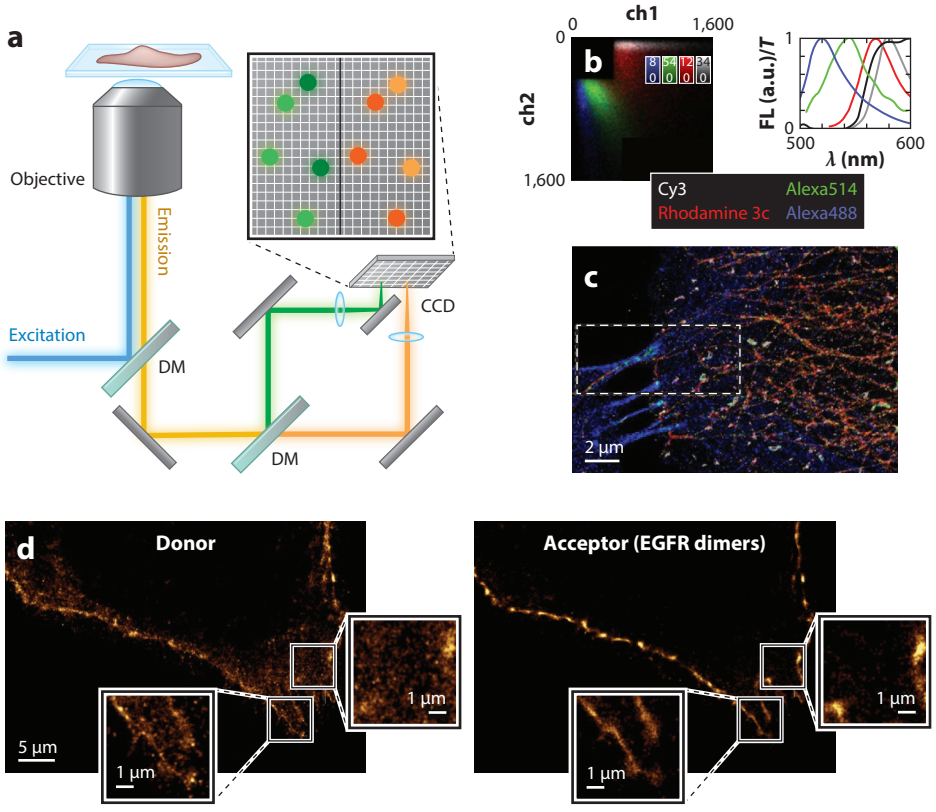

Figure 2

Wavelength-split detection for multicolor SMLM and smFRET in living cells. (*a*) Schematic of a DM separating long- and short-wavelength components of single-molecule emission for simultaneous imaging on two areas of a CCD. (*b*) Distribution of photon counts in the long- and short-wavelength channels for single molecules detected in SMLM for four dyes with overlapping emission spectra (*graph*). (*c*) Simultaneous four-color SMLM of a fixed cell performed by separating the single-molecule emission of four dyes based on panel *b*. (*d*) SMLM images due to the binding/unbinding of a mixture of donor- and acceptor-labeled EGF molecules to EGFR in the plasma membrane of a live mammalian cell, for the (*left*) donor and (*right*) acceptor channels when exciting the donor. Insets show zoomed-in images of the boxed regions. Single-molecule emission in the acceptor channel is attributed to smFRET between single donor- and acceptor-labeled EGFs bound to an EGFR dimer. Abbreviations: CCD, charge-coupled device; DM, dichroic mirror; EGF, epidermal growth factor; EGFR, epidermal growth factor receptor; FL, fluorescence; smFRET, single-molecule Förster resonance energy transfer; SMLM, single-molecule localization microscopy; T, transmission. Panels *b* and *c* adapted with permission from Reference 39; copyright 2010 Elsevier. Panel *d* adapted from Reference 57 (CC BY-NC-ND 3.0).

devised to introduce organic dye-based smFRET probes into mammalian and bacterial cells, including microinjection (50–52), heat shock (53), and electroporation (54), or by combining FPs with self-labeling tags and fluorogenic membrane-permeable dyes (55). Separately, dye tagging can be more readily achieved for targets at the cell surface (56–58).

With the labeling issues addressed, live-cell smFRET is so far still limited in its spatial mapping capabilities. For example, the formation of SNARE protein complexes in live cells has been examined with wide-field smFRET, but only for ~100 sparsely distributed molecules (51). With confocal smFRET, König et al. (52) monitored the compaction of the intrinsically disordered protein

ProTα in live cells but only demonstrated limited spatial information by distinguishing molecules located in the nucleus, cytosol, and outside the cell. For studying the dimerization of G protein–coupled receptors at the cell surface, Asher et al. (58) recorded long time traces to monitor dimer conformations and intramembrane diffusion, but under either low expression levels or after photobleaching to ensure sparse single molecules. Utilizing the dynamic binding/unbinding of epidermal growth factor (EGF) labeled by donor or acceptor dyes to EGF receptors (EGFRs) at the cell surface, Winckler et al. (57) recorded high-density smFRET in the wide field over $\sim 10^4$ frames, and so obtained SMLM maps of EGFR dimers, showing preferential localization to the cell edge (**Figure 2*d***). However, quantification of such smFRET data is difficult as the stochastic labeling leads to only a small proportion of the dimers containing both the donor and acceptor dyes.

3.2. Spectrally Resolved Single-Molecule Localization Microscopy

Although wavelength-split detection is simple in implementation, it achieves limited spectral sensitivity. The ratiometric readouts calculated from the two split views depend on the spectral characteristics of the dichroic mirror used, and so the results are difficult to compare between studies and are vulnerable to operational conditions, including backgrounds.

To resolve the actual emission spectra of single molecules, typical approaches spatially confine the illumination and/or detection (e.g., to a single spot in a confocal setting) to ensure that fluorescence is spectrally dispersed from only one single molecule at a time (9, 59). Scanning across the sample then maps out the spectra of different molecules. Although good spectra are recorded, such single-spot detection schemes afford low throughput and limit samples to sparse molecules that are resolvable with diffraction-limited optics.

These limitations are overcome by a new detection scheme in which single-molecule fluorescence is dispersed in the wide field (60, 61). For molecules sparsely distributed in each frame, as encountered in SMLM, it is noted that their images are self-confined into individual emission spots. Concurrent spectral dispersion of these point sources in the wide field thus enables the parallel recording of tens of single-molecule spectra with an ~10-ms camera snapshot (**Figure 3*a*,*b***). Next, utilizing single-molecule fluorescence on-off switching to visit different molecules over consecutive camera frames, a key strategy of SMLM, the spectra of millions of single molecules are thus acquired in minutes, hence affording ultrahigh-throughput SMS.

The massively accumulated single-molecule spectra, alongside the concurrently superlocalized positions of the same molecules, are synthesized into spectrally resolved SMLM (SR-SMLM) data affording local emission spectra at nanoscale spatial resolution (15, 60–63). When applied to multiplexed imaging (60, 62–64), such approaches achieved cross talk–free 3D SRM for four fluorophores with heavily overlapping spectra (60) and the simultaneous tracking of different single molecules and quantum dots (64, 65).

Integration with fluorescent probes that exhibit spectral changes in response to local physicochemical parameters next enabled super-resolution functional mapping. With the solvatochromic dye Nile red, SR-SMLM thus resolved nanoscale heterogeneities in the membranes of live mammalian cells, showing the intracellular organelle membranes as chemically more polar than the plasm membrane owing to less ordered lipid packing (**Figure 3*c*,*d***), and noting the formation of low-polarity, raft-like nanodomains in the plasma membrane upon cholesterol addition or cholera-toxin treatment (16). For in vitro systems, Nile red–based SR-SMLM has similarly resolved chemical polarities for model lipid bilayer membranes and vesicles (15, 16, 66), protein aggregates (**Figure 3*e*,*f***) (15, 17, 19), surface adlayers (67), and polymeric nanoparticles (68). A tailor-made Nile red derivative further enabled the specific probing of the live-cell plasma membrane, unveiling nanoscopic protrusions and invaginations of reduced lipid order (**Figure 3*g***) (69).

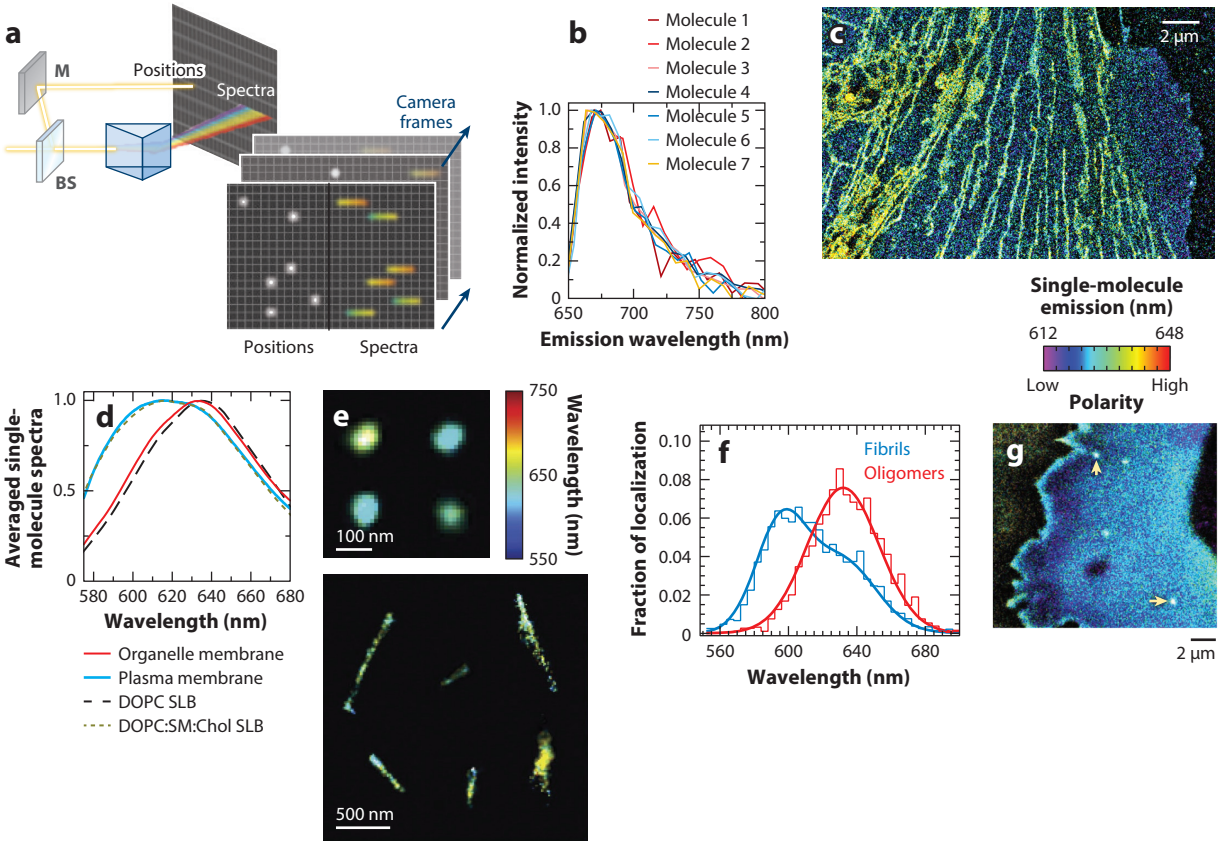

Figure 3

SR-SMLM and super-resolution mapping of chemical polarity for live-cell membranes and in vitro protein aggregates. (*a*) Schematic of fluorescence dispersed in the wide field, so the emission spectra of many single molecules are concurrently captured in a camera frame. Single-molecule fluorescence on-off switching next enables the sampling of different molecules over consecutive frames. (*b*) Example spectra of single Alexa Fluor 647 molecules recorded in a 9-ms camera frame. (*c*) SR-SMLM image of Nile red–highlighted lipid-membrane system in a live mammalian cell. The color presents the single-molecule spectral mean, and longer emission wavelengths correspond to higher local chemical polarities. (*d*) Averaged single-molecule spectra at the plasma membrane versus the internal nanoscale organelle membranes, compared to that at SLBs with and without the packing-order promoter Chol. (*e*) SR-SMLM images of Nile red at the surfaces of in vitro amyloid-β oligomers (*top*) and fibrils (*bottom*). (*f*) Frequency histogram of fluorescence emission peaks for individual Nile red molecules at amyloid-β oligomers and fibrils. (*g*) SR-SMLM image for the plasma membrane of a live mammalian cell labeled by NR4A, a Nile red derivative. Arrows point to higher local chemical polarities at endocytic sites due to reduced lipid order. Abbreviations: BS, beam splitter; Chol, cholesterol; DOPC, 1,2-dioleoyl-*sn*-glycero-3-phosphocholine; M, mirror; SLB, supported lipid bilayer; SR-SMLM, spectrally resolved single-molecule localization microscopy. Panel *b* adapted from Reference 60. Panels *c* and *d* adapted with permission from Reference 16; copyright 2017 American Chemical Society. Panels *e* and *f* adapted from Reference 15 (CC BY 4.0). Panel *g* adapted with permission from Reference 69.

Future SR-SMLM developments may harness the genetic targeting of Nile red (70, 71) to probe specific subcellular targets.

3.3. Excitation-Based Spectral Imaging

Although spectral fluorescence microscopy methods (72, 73), including SR-SMLM, provide powerful paths toward multiplexed and functional imaging, typical approaches of dispersing the local emission are difficult to implement and limit the time resolution.

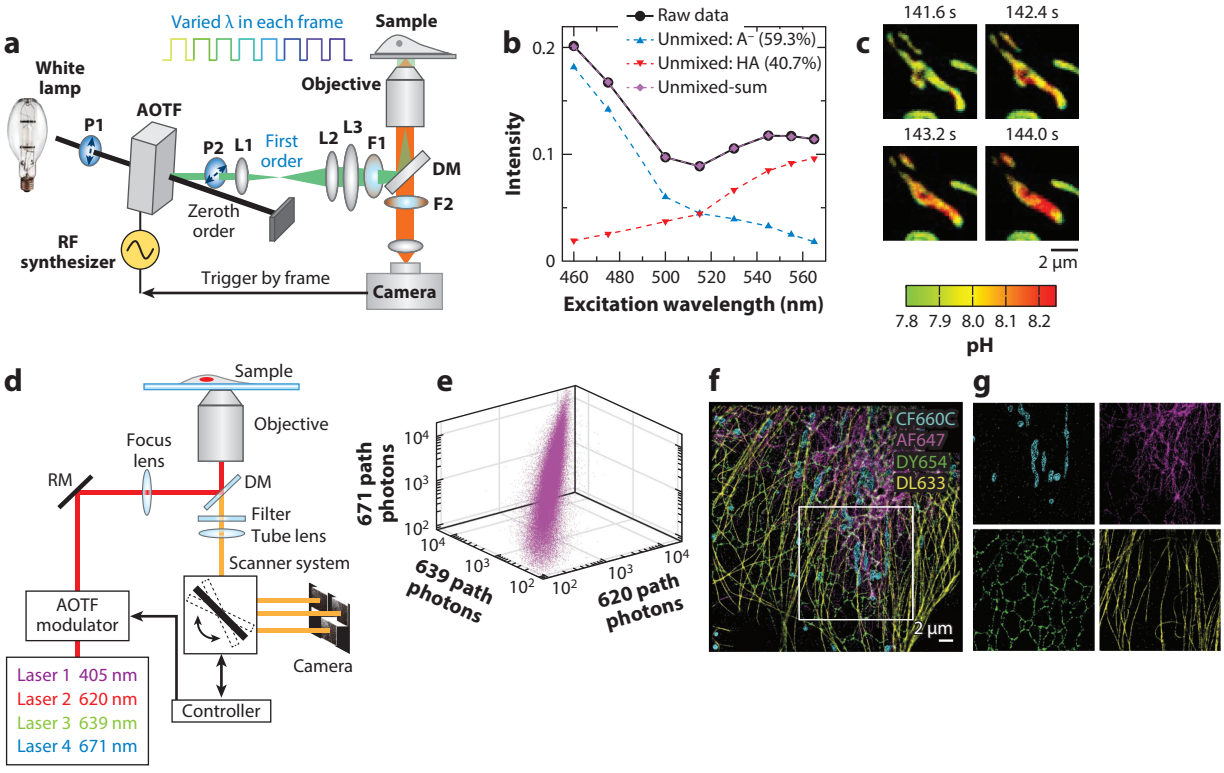

Figure 4

Excitation-based spectral microscopy and application to SMLM. (*a*) Schematic of the setup for varying the excitation wavelength in consecutive frames through the frame-synchronized modulation of the AOTF. (*b*) Eight-wavelength excitation spectrum recorded with the setup in panel *a*, for pHRed FP expressed in a mammalian cell that was equilibrated to pH = 8.0 (*black solid line*), and its linear unmixing into the deprotonated (A^-) and protonated (HA) components (*dashed lines*). (*c*) Color-coded absolute pH map series for pHRed expressed in the mitochondrial matrix in a living mammalian cell, as obtained through the linear unmixing of the excitation spectrum as in panel *b*, showing concurrent fast changes in both the mitochondrial shape and matrix pH at 0.8-s time resolution. (*d*) Schematic for excitation-resolved SMLM. A resonant mirror fast-switches the wide-field image back and forth between three recording positions with synchronized excitation of three lasers of different wavelengths. (*e*) Scatter plot of the photon counts for individual Alexa Fluor 647 molecules when excited by three lasers. (*f*) Tetra-color SMLM by separating the excitation characteristics of four dyes based on their three-excitation-wavelength single-molecule photon counts as shown in panel *e*. (*g*) Separated channels for the box in panel *f*, showing minimal cross talk. Abbreviations: AOTF, acousto-optic tunable filter; DM, dichroic mirror; F, bandpass filter; FP, fluorescent protein; L, lens; P, polarizer; RF, radio frequency; RM, reflective mirror; SMLM, single-molecule localization microscopy. Panels *a–c* adapted from Reference 76 (CC BY 4.0). Panels *d–g* adapted from Reference 78 (CC BY 4.0).

Recent work highlights the power of excitation-based spectral microscopy (74–76). By collecting fluorescence with a fixed emission band but scanning the excitation wavelength for the entire imaging field, such schemes remove the need to disperse the emission signal over many detector pixels (as required in typical emission-based spectral microscopy) yet achieve comparable spectral unmixing capabilities. Thus, with camera frame–synchronized fast scanning of the excitation wavelength (**Figure 4*a***), six subcellular targets, labeled by fluorophores substantially overlapping in spectrum, were simultaneously imaged in the wide field using a single filter cube at low cross talk and high speeds (76). Combining different filter cubes enabled multiplexing with more fluorophores (77). The ability to quantify the abundances of different species via the excitation spectra (**Figure 4*b***) further enabled the fast, quantitative imaging of intracellular physicochemical

parameters, such as pH (**Figure 4*c***) and macromolecular crowding, with bi-state and FRET-based biosensors (76).

The application of excitation-based spectral microscopy to SMLM, however, is nontrivial. As the excitation spectrum is collected by monitoring the emission intensity when the excitation wavelength is scanned, the frequent on-off switching of single-molecule emission in SMLM makes it unreliable, if not impossible, to determine how the emission intensity responds to excitation wavelengths scanned over consecutive camera frames. Wu et al. (78) provided an elegant solution in which a resonant mirror rapidly switched the wide-field image back and forth between three recording positions for many rounds within each camera frame (**Figure 4*d***). With three synchronized excitation lasers, they thus well discriminated four spectrally overlapped fluorophores for the tetra-color SMLM of fixed cells (**Figure 4*e–g***). The potential application of related approaches to living cells and to the functional readouts of fluorescent biosensors presents exciting perspectives.

4. SINGLE-MOLECULE MOTIONS

Motions provide yet another great window into molecular behaviors and interactions. Resolving the intracellular movement of biomolecules may enable the spatial mapping of biophysical parameters, including diffusion modes and constants, viscosity, binding kinetics, and conformational states (79–86).

4.1. Fluorescence Correlation Spectroscopy

Fluorescence correlation spectroscopy (FCS) measures fluorescence fluctuations as single molecules transiently enter and leave the detection spot, e.g., in a confocal setting. By time correlating the detected fluctuations, FCS provides valuable insights into intracellular diffusions, concentrations, and intermolecular interactions (80, 87, 88). Recent integration with stimulated emission depletion (STED) SRM has further pushed FCS beyond the diffraction limit (89). However, single-molecule events are not isolated, and FCS generally achieves limited spatial mapping capabilities (88, 90).

4.2. Single-Particle Tracking

To access motions at the true single-molecule level, single-particle tracking (SPT) has found wide use in living cells and been the subject of many reviews (79, 81, 82, 91). Superlocalizing single molecules enables motion quantification at the nanoscale. Recent advances in MINFLUX, a method that modulates the illumination pattern to achieve photon-efficient localization of single molecules with exceptional spatiotemporal resolutions (92), have permitted the direct observation of a dye-tagged motor protein stepping on intracellular microtubules with <5-nm spatial resolution at few-millisecond temporal resolutions (93). Monitoring the motion of a single molecule over long trajectories further allows the observation of asynchronous dynamics, e.g., transient intermolecular interactions, and the extraction of diverse biophysical parameters such as binding kinetics, non-Brownian diffusion modes, and directional transport (81, 84).

While SPT is traditionally applied to sparse molecules to avoid trajectory overlapping, recent developments integrating SMLM-inspired photoactivation and fluorophore-exchange schemes have permitted the high-density tracking of single-molecule trajectories (57, 91, 94–97). However, the focus is often on obtaining long trajectories to assign a diffusion coefficient value to each molecule, thus yielding limited spatial mapping and restricting applications to slow diffusion in membranes, where the bound molecules stay in focus over many frames.

4.3. Single-Molecule Displacement/Diffusivity Mapping

To overcome SPT's limited spatial mapping capabilities and access the fast diffusion of unbound molecules, an emerging approach, single-molecule displacement/diffusivity mapping (SM*d*M) (98, 99), forgoes trajectories and focuses on transient displacements. Thus, rather than following how each molecule behaves as it randomly visits different, potentially heterogeneous locations, SM*d*M flips the question to survey, for each fixed location, how different (yet identical) single molecules move locally. This location-centered strategy is naturally powerful for spatial mapping. Moreover, by focusing on transient displacements, each molecule only needs to be localized twice within a short time window. For fast-diffusing molecules, a tandem excitation scheme is thus devised to apply a pair of closely timed stroboscopic pulses across two camera frames to capture single-molecule images over time separations substantially shorter than the camera frame time, from which single-molecule displacements are extracted (**Figure 5*a*,*b***) (98). This tandem excitation scheme further

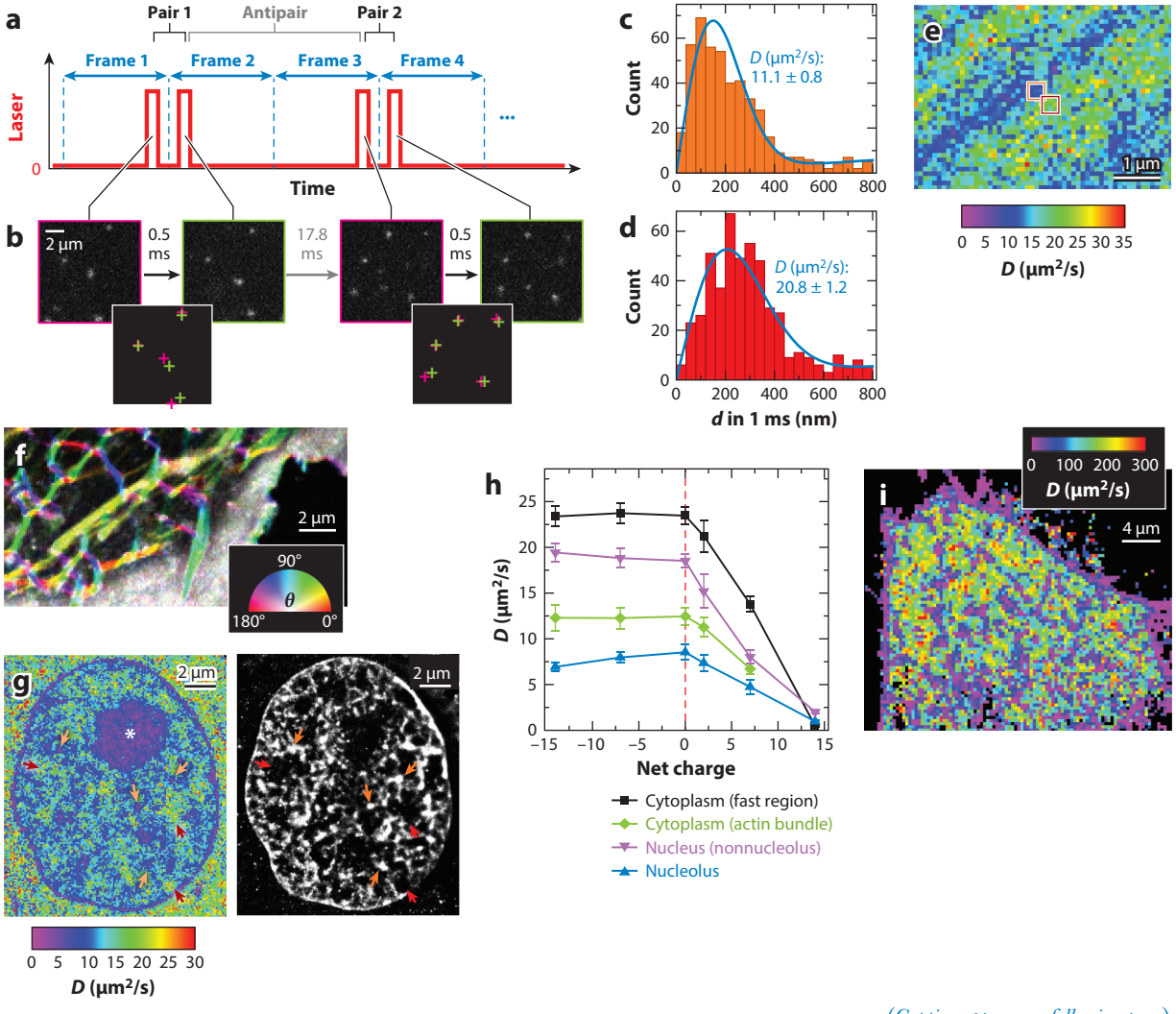

(*Caption appears on following page*)

Figure 5 (*Figure appears on preceding page*)

SM*d*M provides super-resolution mapping of fast intracellular diffusion. (*a*) Schematic showing a pair of closely timed stroboscopic excitation pulses, which are applied across two tandem camera frames so that the two recorded images correspond to the short time separation Δt between the paired pulses. This paired excitation scheme is repeated $\sim 10^4$ times to enable statistics. (*b*) Example single-molecule images of sulforhodamine 101 molecules diffusing in a living rat astrocyte, recorded in four consecutive frames with the tandem excitation scheme shown in panel *a*. Here, each pulse lasted 200 μs, the center-to-center separation between paired pulses was $\Delta t = 500$ μs, and the camera frame time was 9.15 ms. (*Insets*) Comparison of the localized single-molecule positions across the tandem frames, from which single-molecule displacements are extracted. (*c*,*d*) Distributions of displacements in $\Delta t = 1$ ms for single mEos3.2 FP molecules in a living mammalian cell for two adjacent 300 × 300–nm^2 areas marked with orange and red boxes in panel *e*. Blue curves show fits to a diffusion model, with resultant *D* values labeled. (*e*) Color-coded SM*d*M *D* map for the intracellular diffusion of mEos3.2, obtained by spatially binning the accumulated single-molecule displacements onto 100 × 100–nm^2 grids for local fitting as in panels *c* and *d*. (*f*) Color map presenting the SM*d*M-determined local principal direction of diffusion for BDP-TMR-alkyne in cellular membranes, showing anisotropic diffusion along the endoplasmic reticulum tubules. (*g*) SM*d*M *D* map for mEos3.2 FP in the nuclear region of a living mammalian cell (*left*) versus SMLM of the same region with a DNA stain (*right*), showing reduced *D* in the nucleolus (*asterisk*) and fast and slow diffusion regions correlating to low and high local DNA densities (*red* and *orange arrows*). (*h*) SM*d*M-determined mean *D* values for mEos3.2 FPs of different net charges in different subcellular environments. (*i*) SM*d*M *D* map of Cy3B dye in a living mammalian cell, obtained with $\Delta t = 400$ μs. Abbreviations: FP, fluorescent protein; SM*d*M, single-molecule displacement/diffusivity mapping. Panel *b* adapted with permission from Reference 100; copyright 2023 American Chemical Society. Panels *c*–*e* adapted from Reference 98. Panel *f* adapted with permission from Reference 99; copyright 2020 American Chemical Society. Panels *g* and *h* adapted from Reference 98. Panel *i* adapted with permission from Reference 100; copyright 2023 American Chemical Society.

leaves ample time between the antipaired pulses (**Figure 5*a*,*b***) to allow efficient probe exchanges through diffusion, thus enabling SM*d*M for nonphotoswitchable fluorophores (98, 100). Repeating the above scheme $\sim 10^4$ times accumulates millions of single-molecule displacements to be spatially binned for individual fitting to assess the local diffusion coefficient *D* (**Figure 5*c*,*d***) and generate its super-resolved map (**Figure 5*e***) (98). Local displacement direction analysis is further developed to elucidate diffusion anisotropy (**Figure 5*f***) (99, 101).

With ∼30-kDa FPs, SM*d*M thus uncovered nanoscale diffusion heterogeneities in the mammalian cytoplasm (**Figure 5*e***), nucleus (**Figure 5*g***), and organelles, and identified the protein net charge as a key determinant of intracellular diffusion (**Figure 5*h***) (98, 101). By squeezing the tandem-pulse time separation to 400 μs and incorporating graphene-based electroporation for probe delivery (102), SM*d*M further quantified the very fast diffusion of small (<1 kDa) solutes, unveiling their unhindered diffusion in the mammalian cell (**Figure 5*i***) (100). For cellular membranes, integration of SM*d*M with Nile red–based SR-SMLM resolved diffusion heterogeneities of different origins (99). For in vitro FUS condensates formed through liquid-liquid phase separation, SM*d*M unveiled substantial diffusion slowdowns at surface nanoaggregates (19).

The massively accumulated single-molecule displacements in SM*d*M further enable *D*-value determination to ±1% precisions (103), which has been utilized to establish a universal dependency of *D* on molecular weight for proteins and small molecules (102, 103), show no changes in *D* in enzyme reactions (103), and determine how *D* scales with meshwork sizes in expandable hydrogels (104).

While SM*d*M of FPs in mammalian cells has so far focused on elucidating nonspecific charge interactions, tagging FPs to specific intracellular proteins could employ SM*d*M to map intracellular protein conformation, oligomerization, and interactions; recent SM*d*M work on bacteria has pointed to such directions (105, 106). The compatibility of SM*d*M with nonphotoswitchable fluorophores (98, 100) and the demonstrated successful intracellular probe delivery for SM*d*M (100) further imply the possible integration of SM*d*M with the above-discussed dye-based smFRET for functional readouts. Meanwhile, while SM*d*M has unveiled rich diffusion heterogeneity by just analyzing single-step displacements between tandem frames, future developments may expand on this concept to enable the detection of few-step short tracks, from which one may garner information on nonlinear diffusion and dynamic transition between states.

5. SINGLE-MOLECULE FLUORESCENCE POLARIZATION AND ANISOTROPY

Fluorescence polarization and anisotropy offer valuable information about molecular orientations and dynamics (107, 108). Splitting the fluorescence emission into orthogonal polarizations and/or modulating the polarization orientation of the excitation laser enables the encoding/decoding of single-molecule polarization and anisotropy in SMLM (109–112).

Biological filaments are often assembled from oriented subunits. For in vitro samples, the fixed binding orientations of fluorogenic probes to filaments have thus mapped molecular orientations for DNA strands (111–113) and amyloid fibrils (18, 21) in polarization-resolved SMLM data. For imaging in the mammalian cell, early studies examined fluorescence anisotropy in the SMLM data of FP-tagged actin to detect local heterogeneity in rotational mobility (109, 110). Valades Cruz et al. (112) compared polarization-resolved SMLM data for differently labeled microtubule and actin cytoskeletons in fixed cells and identified Alexa Fluor 488 phalloidin as a good probe to resolve the orientation of the latter. By delivering the same probe into live mammalian cells at low concentrations, Mehta et al. (114) resolved actin filament orientations in SPT to compare with the retrograde flow direction at the leading edge. Rimoli et al. (115) recently developed strategies to determine single molecules' orientation in two dimensions and infer their 3D orientations, which they applied to the SMLM of Alexa Fluor 488 phalloidin–labeled dense actin structures in fixed cells (**Figure 6*a–d***).

Polarization-based functional SMLM has also shed new light on the structure of lipid membranes. Integrating polarized beam splitting and a spatial light modulator, Lu et al. (116) encoded 3D orientation and wobbling into the single-molecule point spread function and thus analyzed the ordering and packing effects of cholesterol in supported lipid bilayers and resolved nanoscale domains with different ordering parameters. A recent study constructed a radially and azimuthally polarized multiview reflector to image single-molecule fluorescence across eight polarization channels to simultaneously determine molecular location and orientation in three dimensions each, and the resultant 6D SMLM resolved dye orientations in fixed-cell membranes (**Figure 6*e–f***) (117).

6. SINGLE-MOLECULE FLUORESCENCE LIFETIME

By detecting the exponential decay rate of emission at the nanosecond timescale, fluorescence lifetime imaging microscopy provides a powerful, probe concentration-insensitive handle for the functional imaging of biological samples (118–120), with diverse probes developed for chemical polarity, viscosity, temperature, and different analytes.

Fluorescence lifetime-resolved SMLM (FL-SMLM) has been achieved with both confocal and wide-field experimental setups (**Figure 7*a–d***), utilizing a single-element single-photon avalanche diode detector and an array detector based on a microchannel-plate photomultiplier tube, respectively (121, 122). Whereas confocal setups can only image a relatively small field of view with reasonable imaging speeds, the currently available array detectors suffer from low (∼5%) quantum efficiencies. Lifetime estimations can also be made for the wide field with conventional high-sensitivity cameras by time gating the signal electro-optically with a Pockels cell (**Figure 7*e*,*f***) (123), but with limitations on sensitivity.

Thus far, the application of FL-SMLM has been limited to in vitro samples and fixed cells, with an initial focus on separating labels for multiplexed imaging (**Figure 7*b*,*c*,*f***) (121, 122, 124). Recent work detected FRET (125) and metal/graphene-induced energy transfer (122, 126, 127), the latter further enabling 3D SMLM by providing an interesting way to determine the fluorophore's distance to the substrate (**Figure 7*d***). Possible future FL-SMLM applications to live

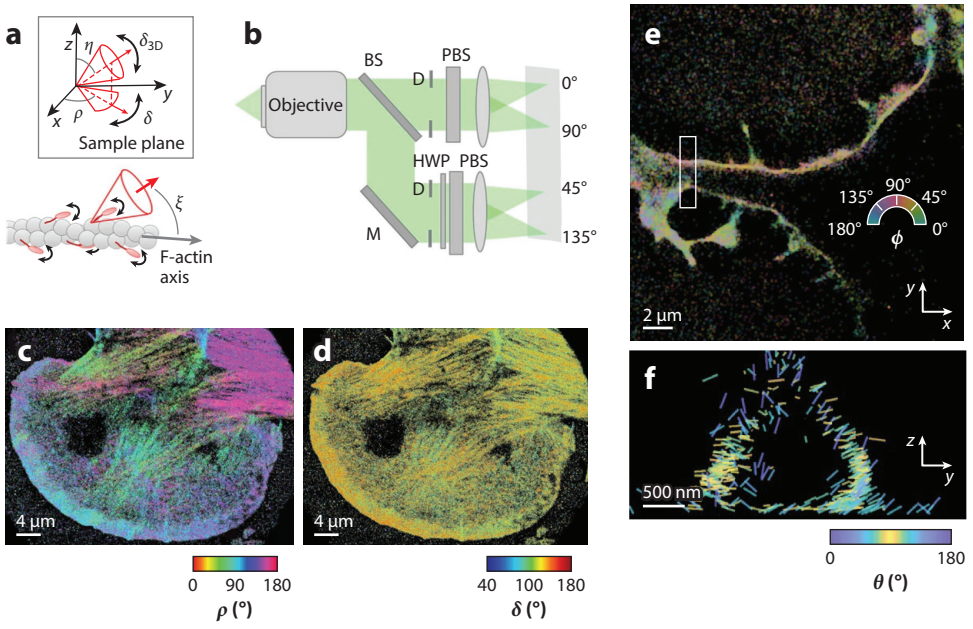

Figure 6

Polarization-resolved SMLM and its applications to the cytoskeleton and membrane in fixed cells. (*a*) Schematic of the fluorescence polarization behavior of Alexa Fluor 488 phalloidin labeling an actin filament. (*b*) Schematic of the extraction of single-molecule fluorescence polarization orientation and wobbling by reducing the detection numerical aperture with D and combining an HWP and two PBSs. (*c*,*d*) Resultant SMLM images resolving the mean orientation (*c*) and wobbling angle (*d*) of Alexa Fluor 488 phalloidin labeling the actin cytoskeleton in a fixed cell. (*e*,*f*) 6D (3D spatial and 3D orientational) SMLM imaging of merocyanine 540 molecules bound to the membrane of a fixed cell: (*e*) In plane (*x*-*y*) view, colored by the single-molecule azimuthal angle ϕ, and (*f*) vertical (*y*-*z*) view of the boxed region, colored by the single-molecule polar angle θ. Abbreviations: BS, beam splitter; D, diaphragm; HWP, half-wave plate; M, mirror; PBS, polarizing beam splitter; SMLM, single-molecule localization microscopy. Panels *a*–*d* adapted from Reference 115 (CC BY 4.0). Panels *e* and *f* adapted with permission from Reference 117.

cells and to the super-resolution mapping of local environments and intermolecular interactions hold great potential.

7. NONFLUORESCENCE METHODS

The above success of SMLM for functional SRM imaging raises the question of whether related approaches could be applied to nonfluorescence methods, which may overcome the limited number of photons that can be extracted from individual fluorophores, enable label-free imaging, or access new spectroscopy insights for decoding physicochemical parameters (128–130).

Microspheres and nanoparticles have long served as unbleachable probes for live-cell SPT (91, 131). Recent advances in photothermal microscopy (91, 128, 132) and interferometric scattering microscopy (133–136) have further enabled the SPT of small gold nanoparticles in live cells, as well as the room-temperature detection and analysis of single molecules in vitro. It, however, remains a challenge to resolve single molecules in the crowded cell or to detect many molecules within the diffraction limit.

Nonlinear optical methods such as nonlinear Raman, harmonic generation, multiphoton fluorescence, and transient absorption offer intriguing prospects for functional SRM for their

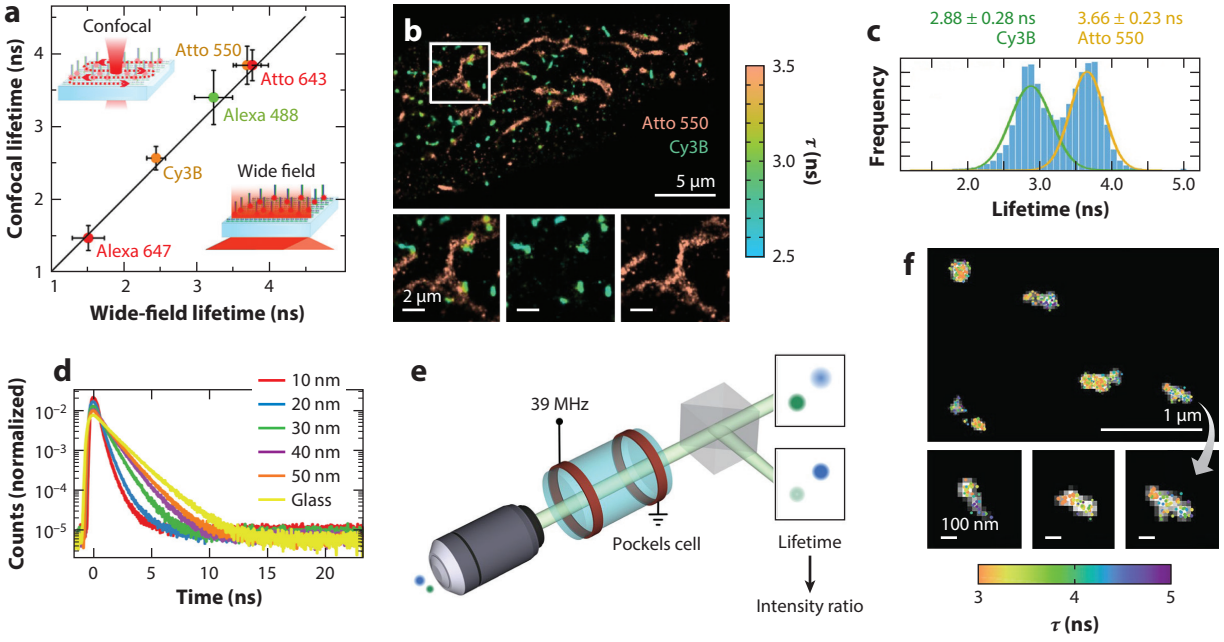

Figure 7

Fluorescence lifetime-resolved SMLM. (*a*) Comparison of the fluorescence lifetime of single molecules of five dyes measured with confocal and wide-field SMLM setups. (*b*, *top*) Wide-field lifetime-resolved SMLM image of a fixed cell double labeled with Cy3B against peroxisomes and Atto 550 against mitochondria, with the colors presenting the measured lifetime. (*b*, *bottom*) Close-up of the boxed region and separation of the two dyes based on the lifetime. (*c*) Lifetime histograms corresponding to panel *b*. (*d*) Fluorescence lifetime curves for AF647-DNA molecules on glass and on gold substrates with 10–50-nm-thick SiO_2 spacers measured with confocal lifetime imaging, demonstrating distance-dependent decreases in the fluorescence lifetime owing to metal-induced energy transfer. (*e*) Schematic of time-gated electro-optic imaging for wide-field lifetime-resolved SMLM using a resonantly driven Pockels cell and a polarizing beam splitter. (*f*) Resultant lifetime-resolved SMLM image of DNA origamis labeled with Cy3B and Atto 565. Abbreviation: SMLM, single-molecule localization microscopy. Panels *a–c* adapted from Reference 122 (CC BY-NC-ND 4.0). Panel *d* adapted from Reference 126 (CC BY-NC 4.0). Panels *e* and *f* adapted with permission from Reference 123; copyright 2021 American Chemical Society.

outstanding chemical and structural contrasts (130, 137–139). Super-resolution nonlinear optical microscopy has been achieved with expansion microscopy (140, 141), STED-based imaging (142), and interferometric excitation (143), among other approaches (129, 130). Application to SMLM is limited by the relatively low probability of nonlinear optical processes and the need for a scalable approach to signal modulation for the isolation of single molecules. Plasmonic amplification of light-matter interactions (144) provides a viable path; surface-enhanced Raman spectroscopy has achieved single-molecule sensitivity (145, 146), and its local blinking has enabled SMLM-type imaging of dried samples (147, 148). However, the patterned plasmonic substrates distort the resultant image, and their required proximity to the sample limits applicability.

8. CONCLUSION

In conclusion, while the outstanding spatial resolution of SMLM has attracted wide attention, in this review we showcased how, by extending mass-accumulated single-molecule measurements to higher dimensions, including emission and excitation spectra, motion, polarization, and fluorescence lifetime, the resultant multidimensional SRM approaches provide fascinating new insights into physicochemical parameters in the living cell.

Future developments call for a synergy of continued innovations in optics on both the excitation and detection fronts, fluorescent probe design, synthesis, and delivery methods, as well as algorithm and analysis tools. The need to detect single molecules and invoke fluorescence on-off switching poses significant challenges: Optimal results thus demand bright probes with high fluorescence quantum yields, while on-off mechanisms such as photoswitching or reversible binding often need to be built in. Yet, the uniqueness of sparse molecules across the camera frame, as often achieved in SMLM, offers new possibilities, so that single-molecule images may be directly stretched/dispersed in the wide field for high-throughput recording, and the recorded signal from each molecule is guaranteed a single identity, removing the need for unmixing. New illumination sequences further enable SMLM/SM*d*M for constantly bright fluorophores via diffusion-based probe exchange. Integrations between different SMLM modules, as well as correlative approaches with other microscopy and spectroscopy techniques (149), provide additional opportunities.

DISCLOSURE STATEMENT

The authors are not aware of any affiliations, memberships, funding, or financial holdings that might be perceived as affecting the objectivity of this review.

ACKNOWLEDGMENTS

We acknowledge support from the National Institute of General Medical Sciences of the National Institutes of Health (DP2GM132681 and R35GM149349), the National Science Foundation (CHE-2203518), the Packard Fellowships for Science and Engineering, and a Heising-Simons Faculty Fellows Award.

LITERATURE CITED

1. Liu Z, Lavis LD, Betzig E. 2015. Imaging live-cell dynamics and structure at the single-molecule level. *Mol. Cell* 58:644–59
2. Sahl SJ, Hell SW, Jakobs S. 2017. Fluorescence nanoscopy in cell biology. *Nat. Rev. Mol. Cell Biol.* 18:685–701
3. Sigal YM, Zhou R, Zhuang X. 2018. Visualizing and discovering cellular structures with super-resolution microscopy. *Science* 361:880–87
4. Möckl L, Moerner WE. 2020. Super-resolution microscopy with single molecules in biology and beyond–essentials, current trends, and future challenges. *J. Am. Chem. Soc.* 142:17828–44
5. Lelek M, Gyparaki MT, Beliu G, Schueder F, Griffié J, et al. 2021. Single-molecule localization microscopy. *Nat. Rev. Methods Primers* 1:39
6. Xiang L, Chen K, Xu K. 2021. Single molecules are your quanta: a bottom-up approach toward multidimensional super-resolution microscopy. *ACS Nano* 15:12483–96
7. Yan R, Wang B, Xu K. 2019. *Functional* super-resolution microscopy of the cell. *Curr. Opin. Chem. Biol.* 51:92–97
8. Weiss S. 1999. Fluorescence spectroscopy of single biomolecules. *Science* 283:1676–83
9. Moerner WE, Fromm DP. 2003. Methods of single-molecule fluorescence spectroscopy and microscopy. *Rev. Sci. Instrum.* 74:3597–619
10. Xie XS, Choi PJ, Li GW, Lee NK, Lia G. 2008. Single-molecule approach to molecular biology in living bacterial cells. *Annu. Rev. Biophys.* 37:417–44
11. Joo C, Balci H, Ishitsuka Y, Buranachai C, Ha T. 2008. Advances in single-molecule fluorescence methods for molecular biology. *Annu. Rev. Biochem.* 77:51–76
12. Klymchenko AS. 2017. Solvatochromic and fluorogenic dyes as environment-sensitive probes: design and biological applications. *Acc. Chem. Res.* 50:366–75
13. Sharonov A, Hochstrasser RM. 2006. Wide-field subdiffraction imaging by accumulated binding of diffusing probes. *PNAS* 103:18911–16

14. Lew MD, Lee SF, Ptacin JL, Lee MK, Twieg RJ, et al. 2011. Three-dimensional superresolution colocalization of intracellular protein superstructures and the cell surface in live *Caulobacter crescentus*. *PNAS* 108:E1102–10
15. Bongiovanni MN, Godet J, Horrocks MH, Tosatto L, Carr AR, et al. 2016. Multi-dimensional super-resolution imaging enables surface hydrophobicity mapping. *Nat. Commun.* 7:13544
16. Moon S, Yan R, Kenny SJ, Shyu Y, Xiang L, et al. 2017. Spectrally resolved, functional super-resolution microscopy reveals nanoscale compositional heterogeneity in live-cell membranes. *J. Am. Chem. Soc.* 139:10944–47
17. Lee JE, Sang JC, Rodrigues M, Carr AR, Horrocks MH, et al. 2018. Mapping surface hydrophobicity of α-synuclein oligomers at the nanoscale. *Nano Lett.* 18:7494–501
18. Ding T, Wu T, Mazidi H, Zhang O, Lew MD. 2020. Single-molecule orientation localization microscopy for resolving structural heterogeneities between amyloid fibrils. *Optica* 7:602–7
19. He C, Wu CY, Li W, Xu K. 2023. Multidimensional super-resolution microscopy unveils nanoscale surface aggregates in the aging of FUS condensates. *J. Am. Chem. Soc.* 145:24240–48
20. Ries J, Udayar V, Soragni A, Hornemann S, Nilsson KP, et al. 2013. Superresolution imaging of amyloid fibrils with binding-activated probes. *ACS Chem. Neurosci.* 4:1057–61
21. Shaban HA, Valades-Cruz CA, Savatier J, Brasselet S. 2017. Polarized super-resolution structural imaging inside amyloid fibrils using Thioflavine T. *Sci. Rep.* 7:12482
22. Needham LM, Weber J, Varela JA, Fyfe JWB, Do DT, et al. 2020. ThX – a next-generation probe for the early detection of amyloid aggregates. *Chem. Sci.* 11:4578–83
23. Torra J, Viela F, Megias D, Sot B, Flors C. 2022. Versatile near-infrared super-resolution imaging of amyloid fibrils with the fluorogenic probe CRANAD-2. *Chemistry* 28:e202200026
24. Morten MJ, Sirvio L, Rupawala H, Mee Hayes E, Franco A, et al. 2022. Quantitative super-resolution imaging of pathological aggregates reveals distinct toxicity profiles in different synucleinopathies. *PNAS* 119:e2205591119
25. Liu B, Stone OJ, Pablo M, Herron JC, Nogueira AT, et al. 2021. Biosensors based on peptide exposure show single molecule conformations in live cells. *Cell* 184:5670–85
26. Chan J, Dodani SC, Chang CJ. 2012. Reaction-based small-molecule fluorescent probes for chemoselective bioimaging. *Nat. Chem.* 4:973–84
27. Halabi EA, Thiel Z, Trapp N, Pinotsi D, Rivera-Fuentes P. 2017. A photoactivatable probe for super-resolution imaging of enzymatic activity in live cells. *J. Am. Chem. Soc.* 139:13200–7
28. Chai X, Han HH, Sedgwick AC, Li N, Zang Y, et al. 2020. Photochromic fluorescent probe strategy for the super-resolution imaging of biologically important biomarkers. *J. Am. Chem. Soc.* 142:18005–13
29. Tang AH, Chen H, Li TP, Metzbower SR, MacGillavry HD, Blanpied TA. 2016. A trans-synaptic nanocolumn aligns neurotransmitter release to receptors. *Nature* 536:210–14
30. Ellefsen KL, Holt JR, Chang AC, Nourse JL, Arulmoli J, et al. 2019. Myosin-II mediated traction forces evoke localized Piezo1-dependent Ca^{2+} flickers. *Commun. Biol.* 2:298
31. Newman ZL, Bakshinskaya D, Schultz R, Kenny SJ, Moon S, et al. 2022. Determinants of synapse diversity revealed by super-resolution quantal transmission and active zone imaging. *Nat. Commun.* 13:229
32. Zhao Y, Pal K, Tu Y, Wang X. 2020. Cellular force nanoscopy with 50 nm resolution based on integrin molecular tension imaging and localization. *J. Am. Chem. Soc.* 142:6930–34
33. Brockman JM, Su H, Blanchard AT, Duan Y, Meyer T, et al. 2020. Live-cell super-resolved PAINT imaging of piconewton cellular traction forces. *Nat. Methods* 17:1018–24
34. Nickerson A, Huang T, Lin LJ, Nan X. 2014. Photoactivated localization microscopy with bimolecular fluorescence complementation (BiFC-PALM) for nanoscale imaging of protein-protein interactions in cells. *PLOS ONE* 9:e100589
35. Liu Z, Xing D, Su QP, Zhu Y, Zhang J, et al. 2014. Super-resolution imaging and tracking of protein-protein interactions in sub-diffraction cellular space. *Nat. Commun.* 5:4443
36. Mo GCH, Ross B, Hertel F, Manna P, Yang XX, et al. 2017. Genetically encoded biosensors for visualizing live-cell biochemical activity at super-resolution. *Nat. Methods* 14:427–34
37. Lin W, Mo GCH, Mehta S, Zhang J. 2021. DrFLINC contextualizes super-resolution activity imaging. *J. Am. Chem. Soc.* 143:14951–55

38. Bossi M, Folling J, Belov VN, Boyarskiy VP, Medda R, et al. 2008. Multicolor far-field fluorescence nanoscopy through isolated detection of distinct molecular species. *Nano Lett.* 8:2463–68
39. Testa I, Wurm CA, Medda R, Rothermel E, von Middendorf C, et al. 2010. Multicolor fluorescence nanoscopy in fixed and living cells by exciting conventional fluorophores with a single wavelength. *Biophys. J.* 99:2686–94
40. Gunewardene MS, Subach FV, Gould TJ, Penoncello GP, Gudheti MV, et al. 2011. Superresolution imaging of multiple fluorescent proteins with highly overlapping emission spectra in living cells. *Biophys. J.* 101:1522–28
41. Brasselet S, Moerner WE. 2000. Fluorescence behavior of single-molecule pH-sensors. *Single Mol.* 1:17–23
42. Sun X, Xie J, Xu J, Higgins DA, Hohn KL. 2015. Single-molecule studies of acidity distributions in mesoporous aluminosilicate thin films. *Langmuir* 31:5667–75
43. Algar WR, Hildebrandt N, Vogel SS, Medintz IL. 2019. FRET as a biomolecular research tool – understanding its potential while avoiding pitfalls. *Nat. Methods* 16:815–29
44. Lerner E, Barth A, Hendrix J, Ambrose B, Birkedal V, et al. 2021. FRET-based dynamic structural biology: challenges, perspectives and an appeal for open-science practices. *eLife* 10:e60416
45. Greenwald EC, Mehta S, Zhang J. 2018. Genetically encoded fluorescent biosensors illuminate the spatiotemporal regulation of signaling networks. *Chem. Rev.* 118:11707–94
46. Wu L, Huang C, Emery BP, Sedgwick AC, Bull SD, et al. 2020. Förster resonance energy transfer (FRET)-based small-molecule sensors and imaging agents. *Chem. Soc. Rev.* 49:5110–39
47. Roy R, Hohng S, Ha T. 2008. A practical guide to single-molecule FRET. *Nat. Methods* 5:507–16
48. Lerner E, Cordes T, Ingargiola A, Alhadid Y, Chung S, et al. 2018. Toward dynamic structural biology: two decades of single-molecule Förster resonance energy transfer. *Science* 359:eaan1133
49. Sustarsic M, Kapanidis AN. 2015. Taking the ruler to the jungle: single-molecule FRET for understanding biomolecular structure and dynamics in live cells. *Curr. Opin. Struct. Biol.* 34:52–59
50. Murakoshi H, Iino R, Kobayashi T, Fujiwara T, Ohshima C, et al. 2004. Single-molecule imaging analysis of Ras activation in living cells. *PNAS* 101:7317–22
51. Sakon JJ, Weninger KR. 2010. Detecting the conformation of individual proteins in live cells. *Nat. Methods* 7:203–5
52. König I, Zarrine-Afsar A, Aznauryan M, Soranno A, Wunderlich B, et al. 2015. Single-molecule spectroscopy of protein conformational dynamics in live eukaryotic cells. *Nat. Methods* 12:773–79
53. Fessl T, Adamec F, Polívka T, Foldynová-Trantírková S, Vácha F, Trantírek L. 2012. Towards characterization of DNA structure under physiological conditions in vivo at the single-molecule level using single-pair FRET. *Nucleic Acids Res.* 40:e121
54. Crawford R, Torella JP, Aigrain L, Plochowietz A, Gryte K, et al. 2013. Long-lived intracellular single-molecule fluorescence using electroporated molecules. *Biophys. J.* 105:2439–50
55. Okamoto K, Hibino K, Sako Y. 2020. In-cell single-molecule FRET measurements reveal three conformational state changes in RAF protein. *Biochim. Biophys. Acta Gen. Subj.* 1864:129358
56. Sako Y, Minoghchi S, Yanagida T. 2000. Single-molecule imaging of EGFR signalling on the surface of living cells. *Nat. Cell Biol.* 2:168–72
57. Winckler P, Lartigue L, Giannone G, De Giorgi F, Ichas F, et al. 2013. Identification and super-resolution imaging of ligand-activated receptor dimers in live cells. *Sci. Rep.* 3:2387
58. Asher WB, Geggier P, Holsey MD, Gilmore GT, Pati AK, et al. 2021. Single-molecule FRET imaging of GPCR dimers in living cells. *Nat. Methods* 18:397–405
59. Michalet X, Siegmund OHW, Vallerga JV, Jelinsky P, Millaud JE, Weiss S. 2007. Detectors for single-molecule fluorescence imaging and spectroscopy. *J. Mod. Opt.* 54:239–81
60. Zhang Z, Kenny SJ, Hauser M, Li W, Xu K. 2015. Ultrahigh-throughput single-molecule spectroscopy and spectrally resolved super-resolution microscopy. *Nat. Methods* 12:935–38
61. Yan R, Moon S, Kenny SJ, Xu K. 2018. Spectrally resolved and functional super-resolution microscopy via ultrahigh-throughput single-molecule spectroscopy. *Acc. Chem. Res.* 51:697–705
62. Mlodzianoski MJ, Curthoys NM, Gunewardene MS, Carter S, Hess ST. 2016. Super-resolution imaging of molecular emission spectra and single molecule spectral fluctuations. *PLOS ONE* 11:e0147506

63. Dong B, Almassalha L, Urban BE, Nguyen TQ, Khuon S, et al. 2016. Super-resolution spectroscopic microscopy via photon localization. *Nat. Commun.* 7:12290
64. Huang T, Phelps C, Wang J, Lin LJ, Bittel A, et al. 2018. Simultaneous multicolor single-molecule tracking with single-laser excitation via spectral imaging. *Biophys. J.* 114:301–10
65. Kakizuka T, Ikezaki K, Kaneshiro J, Fujita H, Watanabe TM, Ichimura T. 2016. Simultaneous nano-tracking of multiple motor proteins via spectral discrimination of quantum dots. *Biomed. Opt. Express* 7:2475–93
66. Davis JL, Zhang Y, Yi SJ, Du FF, Song KH, et al. 2020. Super-resolution imaging of self-assembled nanocarriers using quantitative spectroscopic analysis for cluster extraction. *Langmuir* 36:2291–99
67. Xiang L, Wojcik M, Kenny SJ, Yan R, Moon S, et al. 2018. Optical characterization of surface adlayers and their compositional demixing at the nanoscale. *Nat. Commun.* 9:1435
68. Archontakis E, Deng L, Zijlstra P, Palmans ARA, Albertazzi L. 2022. Spectrally PAINTing a single chain polymeric nanoparticle at super-resolution. *J. Am. Chem. Soc.* 144:23698–707
69. Danylchuk DI, Moon S, Xu K, Klymchenko AS. 2019. Switchable solvatochromic probes for live-cell super-resolution imaging of plasma membrane organization. *Angew. Chem. Int. Ed.* 58:14920–24
70. Prifti E, Reymond L, Umebayashi M, Hovius R, Riezman H, Johnsson K. 2014. A fluorogenic probe for SNAP-tagged plasma membrane proteins based on the solvatochromic molecule Nile red. *ACS Chem. Biol.* 9:606–12
71. Pelletier R, Danylchuk DI, Benaissa H, Broch F, Vauchelles R, et al. 2023. Genetic targeting of solvatochromic dyes for probing nanoscale environments of proteins in organelles. *Anal. Chem.* 95:8512–21
72. Garini Y, Young IT, McNamara G. 2006. Spectral imaging: principles and applications. *Cytom. A* 69A:735–47
73. Gao L, Smith RT. 2015. Optical hyperspectral imaging in microscopy and spectroscopy – a review of data acquisition. *J. Biophotonics* 8:441–56
74. Favreau PF, Hernandez C, Heaster T, Alvarez DF, Rich TC, et al. 2014. Excitation-scanning hyperspectral imaging microscope. *J. Biomed. Opt.* 19:046010
75. Valm AM, Cohen S, Legant WR, Melunis J, Hershberg U, et al. 2017. Applying systems-level spectral imaging and analysis to reveal the organelle interactome. *Nature* 546:162–67
76. Chen K, Yan R, Xiang L, Xu K. 2021. Excitation spectral microscopy for highly multiplexed fluorescence imaging and quantitative biosensing. *Light Sci. Appl.* 10:97
77. Chen K, Li W, Xu K. 2022. Super-multiplexing excitation spectral microscopy with multiple fluorescence bands. *Biomed. Opt. Express* 13:6048–60
78. Wu W, Luo S, Fan C, Yang T, Zhang S, et al. 2023. Tetra-color superresolution microscopy based on excitation spectral demixing. *Light Sci. Appl.* 12:9
79. Kusumi A, Tsunoyama TA, Hirosawa KM, Kasai RS, Fujiwara TK. 2014. Tracking single molecules at work in living cells. *Nat. Chem. Biol.* 10:524–32
80. Machan R, Wohland T. 2014. Recent applications of fluorescence correlation spectroscopy in live systems. *FEBS Lett.* 588:3571–84
81. Manzo C, Garcia-Parajo MF. 2015. A review of progress in single particle tracking: from methods to biophysical insights. *Rep. Prog. Phys.* 78:124601
82. Shen H, Tauzin LJ, Baiyasi R, Wang WX, Moringo N, et al. 2017. Single particle tracking: from theory to biophysical applications. *Chem. Rev.* 117:7331–76
83. Lippincott-Schwartz J, Snapp EL, Phair RD. 2018. The development and enhancement of FRAP as a key tool for investigating protein dynamics. *Biophys. J.* 115:1146–55
84. Elf J, Barkefors I. 2019. Single-molecule kinetics in living cells. *Annu. Rev. Biochem.* 88:635–59
85. Mogre SS, Brown AI, Koslover EF. 2020. Getting around the cell: physical transport in the intracellular world. *Phys. Biol.* 17:061003
86. Yu L, Lei Y, Ma Y, Liu M, Zheng J, et al. 2021. A comprehensive review of fluorescence correlation spectroscopy. *Front. Phys.* 9:644450
87. Mütze J, Ohrt T, Schwille P. 2011. Fluorescence correlation spectroscopy in vivo. *Laser Photonics Rev.* 5:52–67

88. Krieger JW, Singh AP, Bag N, Garbe CS, Saunders TE, et al. 2015. Imaging fluorescence (cross-) correlation spectroscopy in live cells and organisms. *Nat. Protoc.* 10:1948–74
89. Sezgin E, Schneider F, Galiani S, Urbancic I, Waithe D, et al. 2019. Measuring nanoscale diffusion dynamics in cellular membranes with super-resolution STED-FCS. *Nat. Protoc.* 14:1054–83
90. Bag N, Wohland T. 2014. Imaging fluorescence fluctuation spectroscopy: new tools for quantitative bioimaging. *Annu. Rev. Phys. Chem.* 65:225–48
91. Cognet L, Leduc C, Lounis B. 2014. Advances in live-cell single-particle tracking and dynamic super-resolution imaging. *Curr. Opin. Chem. Biol.* 20:78–85
92. Balzarotti F, Eilers Y, Gwosch KC, Gynnå AH, Westphal V, et al. 2017. Nanometer resolution imaging and tracking of fluorescent molecules with minimal photon fluxes. *Science* 355:606–12
93. Deguchi T, Iwanski MK, Schentarra E-M, Heidebrecht C, Schmidt L, et al. 2023. Direct observation of motor protein stepping in living cells using MINFLUX. *Science* 379:1010–15
94. Manley S, Gillette JM, Patterson GH, Shroff H, Hess HF, et al. 2008. High-density mapping of single-molecule trajectories with photoactivated localization microscopy. *Nat. Methods* 5:155–57
95. Giannone G, Hosy E, Levet F, Constals A, Schulze K, et al. 2010. Dynamic superresolution imaging of endogenous proteins on living cells at ultra-high density. *Biophys. J.* 99:1303–10
96. Shim SH, Xia C, Zhong G, Babcock HP, Vaughan JC, et al. 2012. Super-resolution fluorescence imaging of organelles in live cells with photoswitchable membrane probes. *PNAS* 109:13978–83
97. El Beheiry M, Dahan M, Masson JB. 2015. InferenceMAP: mapping of single-molecule dynamics with Bayesian inference. *Nat. Methods* 12:594–95
98. Xiang L, Chen K, Yan R, Li W, Xu K. 2020. Single-molecule displacement mapping unveils nanoscale heterogeneities in intracellular diffusivity. *Nat. Methods* 17:524–30
99. Yan R, Chen K, Xu K. 2020. Probing nanoscale diffusional heterogeneities in cellular membranes through multidimensional single-molecule and super-resolution microscopy. *J. Am. Chem. Soc.* 142:18866–73
100. Choi AA, Xiang L, Li W, Xu K. 2023. Single-molecule displacement mapping indicates unhindered intracellular diffusion of small ($\lesssim$1 kDa) solutes. *J. Am. Chem. Soc.* 145:8510–16
101. Xiang L, Yan R, Chen K, Li W, Xu K. 2023. Single-molecule displacement mapping unveils sign-asymmetric protein charge effects on intraorganellar diffusion. *Nano Lett.* 23:1711–16
102. Moon S, Li W, Hauser M, Xu K. 2020. Graphene-enabled, spatially controlled electroporation of adherent cells for live-cell super-resolution microscopy. *ACS Nano* 14:5609–17
103. Choi AA, Park HH, Chen K, Yan R, Li W, Xu K. 2022. Displacement statistics of unhindered single molecules show no enhanced diffusion in enzymatic reactions. *J. Am. Chem. Soc.* 144:4839–44
104. Park HH, Choi AA, Xu K. 2023. Size-dependent suppression of molecular diffusivity in expandable hydrogels: a single-molecule study. *J. Phys. Chem. B* 127:3333–39
105. Śmigiel WM, Mantovanelli L, Linnik DS, Punter M, Silberberg J, et al. 2022. Protein diffusion in *Escherichia coli* cytoplasm scales with the mass of the complexes and is location dependent. *Sci. Adv.* 8:eabo5387
106. Tran BM, Linnik DS, Punter CM, Śmigiel WM, Mantovanelli L, et al. 2023. Super-resolving microscopy reveals the localizations and movement dynamics of stressosome proteins in *Listeria monocytogenes*. *Commun. Biol.* 6:51
107. Jameson DM, Ross JA. 2010. Fluorescence polarization/anisotropy in diagnostics and imaging. *Chem. Rev.* 110:2685–708
108. Shroder DY, Lippert LG, Goldman YE. 2016. Single molecule optical measurements of orientation and rotations of biological macromolecules. *Methods Appl. Fluoresc.* 4:042004
109. Gould TJ, Gunewardene MS, Gudheti MV, Verkhusha VV, Yin SR, et al. 2008. Nanoscale imaging of molecular positions and anisotropies. *Nat. Methods* 5:1027–30
110. Testa I, Schonle A, Middendorff CV, Geisler C, Medda R, et al. 2008. Nanoscale separation of molecular species based on their rotational mobility. *Opt. Express* 16:21093–104
111. Backer AS, Lee MY, Moerner WE. 2016. Enhanced DNA imaging using super-resolution microscopy and simultaneous single-molecule orientation measurements. *Optica* 3:659–66

112. Valades Cruz CA, Shaban HA, Kress A, Bertaux N, Monneret S, et al. 2016. Quantitative nanoscale imaging of orientational order in biological filaments by polarized superresolution microscopy. *PNAS* 113:E820–28
113. Backer AS, Biebricher AS, King GA, Wuite GJL, Heller I, Peterman EJG. 2019. Single-molecule polarization microscopy of DNA intercalators sheds light on the structure of S-DNA. *Sci. Adv.* 5:eaav1083
114. Mehta SB, McQuilken M, La Riviere PJ, Occhipinti P, Verma A, et al. 2016. Dissection of molecular assembly dynamics by tracking orientation and position of single molecules in live cells. *PNAS* 113:E6352–61
115. Rimoli CV, Valades-Cruz CA, Curcio V, Mavrakis M, Brasselet S. 2022. 4polar-STORM polarized super-resolution imaging of actin filament organization in cells. *Nat. Commun.* 13:301
116. Lu J, Mazidi H, Ding T, Zhang O, Lew MD. 2020. Single-molecule 3D orientation imaging reveals nanoscale compositional heterogeneity in lipid membranes. *Angew. Chem. Int. Ed.* 59:17572–79
117. Zhang O, Guo Z, He Y, Wu T, Vahey MD, Lew MD. 2023. Six-dimensional single-molecule imaging with isotropic resolution using a multi-view reflector microscope. *Nat. Photonics* 17:179–86
118. Berezin MY, Achilefu S. 2010. Fluorescence lifetime measurements and biological imaging. *Chem. Rev.* 110:2641–84
119. Sarder P, Maji D, Achilefu S. 2015. Molecular probes for fluorescence lifetime imaging. *Bioconjugate Chem.* 26:963–74
120. Rupsa D, Tiffany MH, Joe TS, Amani AG, Melissa CS. 2020. Fluorescence lifetime imaging microscopy: fundamentals and advances in instrumentation, analysis, and applications. *J. Biomed. Opt.* 25:071203
121. Thiele JC, Helmerich DA, Oleksiievets N, Tsukanov R, Butkevich E, et al. 2020. Confocal fluorescence-lifetime single-molecule localization microscopy. *ACS Nano* 14:14190–200
122. Oleksiievets N, Mathew C, Thiele JC, Gallea JI, Nevskyi O, et al. 2022. Single-molecule fluorescence lifetime imaging using wide-field and confocal-laser scanning microscopy: a comparative analysis. *Nano Lett.* 22:6454–61
123. Bowman AJ, Kasevich MA. 2021. Resonant electro-optic imaging for microscopy at nanosecond resolution. *ACS Nano* 15:16043–54
124. Masullo LA, Steiner F, Zähringer J, Lopez LF, Bohlen J, et al. 2021. Pulsed interleaved MINFLUX. *Nano Lett.* 21:840–46
125. Zaza C, Chiarelli G, Zweifel LP, Pilo-Pais M, Sisamakis E, et al. 2023. Super-resolved FRET imaging by confocal fluorescence-lifetime single-molecule localization microscopy. *Small Methods* 7:2201565
126. Thiele JC, Jungblut M, Helmerich DA, Tsukanov R, Chizhik A, et al. 2022. Isotropic three-dimensional dual-color super-resolution microscopy with metal-induced energy transfer. *Sci. Adv.* 8:eabo2506
127. Zähringer J, Cole F, Bohlen J, Steiner F, Kamińska I, Tinnefeld P. 2023. Combining pMINFLUX, graphene energy transfer and DNA-PAINT for nanometer precise 3D super-resolution microscopy. *Light Sci. Appl.* 12:70
128. Arroyo JO, Kukura P. 2015. Non-fluorescent schemes for single-molecule detection, imaging and spectroscopy. *Nat. Photonics* 10:11–17
129. Leighton RE, Alperstein AM, Frontiera RR. 2022. Label-free super-resolution imaging techniques. *Annu. Rev. Anal. Chem.* 15:37–55
130. Tang M, Han Y, Jia D, Yang Q, Cheng J-X. 2023. Far-field super-resolution chemical microscopy. *Light Sci. Appl.* 12:137
131. Wang G, Stender AS, Sun W, Fang N. 2010. Optical imaging of non-fluorescent nanoparticle probes in live cells. *Analyst* 135:215–21
132. Adhikari S, Spaeth P, Kar A, Baaske MD, Khatua S, Orrit M. 2020. Photothermal microscopy: imaging the optical absorption of single nanoparticles and single molecules. *ACS Nano* 14:16414–45
133. Young G, Kukura P. 2019. Interferometric scattering microscopy. *Annu. Rev. Phys. Chem.* 70:301–22
134. Taylor RW, Mahmoodabadi RG, Rauschenberger V, Giessl A, Schambony A, Sandoghdar V. 2019. Interferometric scattering microscopy reveals microsecond nanoscopic protein motion on a live cell membrane. *Nat. Photonics* 13:480–87
135. Priest L, Peters JS, Kukura P. 2021. Scattering-based light microscopy: from metal nanoparticles to single proteins. *Chem. Rev.* 121:11937–70

136. Dahmardeh M, Mirzaalian Dastjerdi H, Mazal H, Köstler H, Sandoghdar V. 2023. Self-supervised machine learning pushes the sensitivity limit in label-free detection of single proteins below 10 kDa. *Nat. Methods* 20:442–47
137. Zipfel WR, Williams RM, Webb WW. 2003. Nonlinear magic: multiphoton microscopy in the biosciences. *Nat. Biotechnol.* 21:1369–77
138. Min W, Freudiger CW, Lu S, Xie XS. 2011. Coherent nonlinear optical imaging: beyond fluorescence microscopy. *Annu. Rev. Phys. Chem.* 62:507–30
139. Parodi V, Jacchetti E, Osellame R, Cerullo G, Polli D, Raimondi MT. 2020. Nonlinear optical microscopy: from fundamentals to applications in live bioimaging. *Front. Bioeng. Biotechnol.* 8:585363
140. Qian C, Miao K, Lin L-E, Chen X, Du J, Wei L. 2021. Super-resolution label-free volumetric vibrational imaging. *Nat. Commun.* 12:3648
141. Shi L, Klimas A, Gallagher B, Cheng Z, Fu F, et al. 2022. Super-resolution vibrational imaging using expansion stimulated Raman scattering microscopy. *Adv. Sci.* 9:2200315
142. Xiong H, Qian N, Miao Y, Zhao Z, Chen C, Min W. 2021. Super-resolution vibrational microscopy by stimulated Raman excited fluorescence. *Light Sci. Appl.* 10:87
143. Steves MA, Knappenberger KL. 2023. Improving spectral, spatial, and mechanistic resolution using Fourier transform nonlinear optics: a tutorial review. *ACS Phys. Chem. Au* 3:130–42
144. Wang M, Li M, Jiang S, Gao J, Xi P. 2020. Plasmonics meets super-resolution microscopy in biology. *Micron* 137:102916
145. Zrimsek AB, Chiang N, Mattei M, Zaleski S, McAnally MO, et al. 2017. Single-molecule chemistry with surface- and tip-enhanced Raman spectroscopy. *Chem. Rev.* 117:7583–613
146. Itoh T, Procházka M, Dong Z-C, Ji W, Yamamoto YS, et al. 2023. Toward a new era of SERS and TERS at the nanometer scale: from fundamentals to innovative applications. *Chem. Rev.* 123:1552–634
147. Ayas S, Cinar G, Ozkan AD, Soran Z, Ekiz O, et al. 2013. Label-free nanometer-resolution imaging of biological architectures through surface enhanced Raman scattering. *Sci. Rep.* 3:2624
148. Olson AP, Ertsgaard CT, Elliott SN, Lindquist NC. 2016. Super-resolution chemical imaging with plasmonic substrates. *ACS Photonics* 3:329–36
149. Hauser M, Wojcik M, Kim D, Mahmoudi M, Li W, Xu K. 2017. Correlative super-resolution microscopy: new dimensions and new opportunities. *Chem. Rev.* 117:7428–56